



Search for Large-scale Anisotropy in the Arrival Direction of Cosmic Rays with KASCADE-Grande

W. D. Apel¹, J. C. Arteaga-Velázquez², K. Bekk¹, M. Bertaini³, J. Blümer^{1,4,15}, R. Bonino³, H. Bozdog¹, I. M. Brancus^{5,16}, E. Cantoni^{3,17}, A. Chiavassa³, F. Cossavella^{4,18}, K. Daumiller¹, V. de Souza⁶, F. Di Piero⁷, P. Doll¹, R. Engel¹, D. Fuhrmann^{8,19}, A. Gherghel-Lascu⁵, H. J. Gils¹, R. Glasstetter⁸, C. Grupen⁹, A. Haungs¹, D. Heck¹, J. R. Hörandel¹⁰, T. Huege¹, K.-H. Kampert⁸, D. Kang¹, H. O. Klages¹, K. Link¹, P. Łuczak¹¹, H. J. Mathes¹, H. J. Mayer¹, J. Milke¹, B. Mitrica^{5,16}, C. Morello¹², J. Oehlschläger¹, S. Ostapchenko¹³, T. Pierog¹, H. Rebel¹, M. Roth¹, H. Schieler¹, S. Schöo^{1,20}, F. G. Schröder¹, O. Sima¹⁴, G. Toma⁵, G. C. Trinchero¹², H. Ulrich¹, A. Weindl¹, J. Wochele¹, and J. Zabierowski¹¹

¹Institut für Kernphysik, KIT—Karlsruher Institute für Technologie, Germany; andrea.chiavassa@unito.it

²Institute of Physics and Mathematics, Universidad Michoacana de San Nicolás de Hidalgo, Morelia, Mexico

³Dipartimento di Fisica, Università degli Studi di Torino, Italy

⁴Institut für Experimentelle Teilchenphysik, KIT—Karlsruher Institut für Technologie, Germany

⁵Horia Hulubei National Institute of Physics and Nuclear Engineering, Bucharest, Romania

⁶Universidade de São Paulo, Instituto de Física de São Carlos, Brasil

⁷Istituto Nazionale di Fisica Nucleare, Sezione di Torino, Italy

⁸Fachbereich Physik, Universität Wuppertal, Germany

⁹Department of Physics, Siegen University, Germany

¹⁰Department of Astrophysics, Radboud University Nijmegen, The Netherlands

¹¹National Centre for Nuclear Research, Department of Astrophysics, Łódź, Poland

¹²Osservatorio Astrofisico di Torino, INAF Torino, Italy

¹³Frankfurt Institute for Advanced Studies (FIAS), Frankfurt am Main, Germany

¹⁴Department of Physics, University of Bucharest, Bucharest, Romania

Received 2018 August 23; revised 2018 November 6; accepted 2018 November 15; published 2019 January 11

Abstract

We present the results of the search for large-scale anisotropies in the arrival directions of cosmic rays performed with the KASCADE-Grande experiment at energies higher than 10^{15} eV. To eliminate spurious anisotropies due to atmospheric or instrumental effects we apply the east–west method. We show, using the solar time distribution of the number of counts, that this technique allow us to remove correctly the count variations not associated to real anisotropies. By applying the east–west method we obtain the distribution of number of counts in intervals of 20 minutes of sidereal time. This distribution is then analyzed by searching for a dipole component; the significance of the amplitude of the first harmonic is 3.5σ , therefore, we derive its upper limit. The phase of the first harmonic is determined with an error of a few hours and is in agreement with the measurements obtained in the $10^{14} < E < 2 \times 10^{15}$ eV energy range by the EAS-TOP, IceCube, and IceTop experiments. This supports the hypothesis of a change of the phase of the first harmonic at energies greater than $\sim 2 \times 10^{14}$ eV.

Key words: astroparticle physics – cosmic rays

1. Introduction

Recent measurements of the cosmic-ray spectrum in the energy range around the knee have shown that this feature can be attributed to the light primaries (H or He; Antoni et al. 2002; Aglietta et al. 2004), while the spectrum of heavier elements shows the same feature at higher energies (Apel et al. 2011). These results have been obtained by high-precision EAS (Extensive Air Showers) experiments separating events in two mass groups: light and heavy primaries. The spectrum of the light component measured by the ARGO-YBJ experiment

(Bartoli et al. 2015a) shows a change of the slope at somehow lower energies (700 TeV), hinting at a more complex structure of the spectra than simple power laws. However, all results show that the energy of the change of the slope of the spectrum increases proportionally to the charge of the primary particle. The simplest explanation of these results is the containment of primary particles inside magnetic fields, but spectral measurements cannot discriminate between a containment inside the acceleration region, limiting the maximum achievable energy, or to a containment inside the propagation region. A measurement that could help separate these two scenarios is the search for large-scale anisotropies in the arrival direction of primary cosmic rays. The optimum procedure would be perform such measurement separating events into mass groups. However this requires very large, active areas of about 1 km^2 , multicomponent, high-resolution arrays. None of the experiments that have operated so far satisfy all of the requirements together.

In the 1–20 TeV energy range different experiments, such as Tibet-III (Amenomori et al. 2005), MILAGRO (Abdo et al. 2009), ARGO-YBJ (Bartoli et al. 2015b), and IceCube (Abbasi et al. 2010), detected both large-scale and small-scale anisotropies. At higher energies statistically significant detection of a large-scale

¹⁵ Now: Head of Division V at KIT—Karlsruher Institut für Technologie, Germany.

¹⁶ Deceased.

¹⁷ Now at: Istituto Nazionale di Ricerca Metrologica, INRIM, Torino, Italy.

¹⁸ Now at: DLR Oberpfaffenhofen, Germany.

¹⁹ Now at: University of Duisburg-Essen, Duisburg, Germany.

²⁰ Now at: Siemens AG, Germany.



anisotropy has been claimed by the EAS-TOP (Aglietta et al. 2009), ARGO-YBJ (Bartoli et al. 2018), IceCube (Abbasi et al. 2012), and IceTop (Aartsen et al. 2013) experiments, and at $E > 8 \times 10^{18}$ eV by the Pierre Auger Observatory (Aab et al. 2017).

The search for large-scale anisotropies is performed by EAS experiments through the distribution of the number of events versus sidereal²¹ or solar time, but the counting rates of EAS experiments are affected by instrumental and atmospheric effects (such as pressure or temperature variations) that often are order of magnitudes larger than those expected by cosmic-ray anisotropies. Various methods have been proposed to take into account these variations. The KASCADE-Grande data have been analyzed applying the east–west (Bonino et al. 2011) method: an algorithm based on the counting rate differences between eastward and westward directions; we briefly remind its main points.

The number of counts measured from the east and from the west sectors, at a given time t , are $I_E(t)$ and $I_W(t)$, respectively. Their difference is a measurement of the first derivative of the total number of counts ($I_{\text{tot}}(t)$):

$$\frac{dI_{\text{tot}}}{dt} = \frac{I_E(t) - I_W(t)}{\delta t} = \frac{D(t)}{\delta t}, \quad (1)$$

where δt is the average hour angle between the vertical and the two sectors. Using the Fourier formalism $D(t)$ can be written as:

$$D(i) = a_0 + \sum_{k=1}^{\infty} r_k \cos\left(\frac{2\pi k(i - 1/2)}{n_{\text{int}}} - \psi_k\right), \quad (2)$$

where the 24 hr in solar, sidereal, or anti-sidereal times are divided in n_{int} intervals. The differential amplitude (r_D) and phase (ψ_D) of the first harmonic ($D(t) = r_D \cos(t - \psi_D)$) are obtained by fitting the distribution of the counts difference between the two sectors.

To calculate the expected modulation due to a cosmic-ray anisotropy we integrate the expression of dI_{tot}/dt :

$$I_{\text{tot}}(t) = \int \frac{D(t^*)}{\delta t} dt^* = \frac{r_D}{\delta t} \cos\left(t - \psi_D - \frac{\pi}{2}\right). \quad (3)$$

We then derive the so called true total intensity²² by adding the mean counting rate:

$$I_{\text{tot}}(t) = \langle I \rangle + I(t), \quad (4)$$

with the integral amplitude and phase being:

$$r_I = \frac{r_D}{\delta t},$$

$$\psi_I = \psi_D + \frac{\pi}{2}.$$

²¹ Sidereal time: a common timescale among astronomers that is based on the Earth's rotation measured relative to the fixed stars.

²² By true total intensity we mean the total cosmic-ray counting rate once the spurious fluctuations have been subtracted.

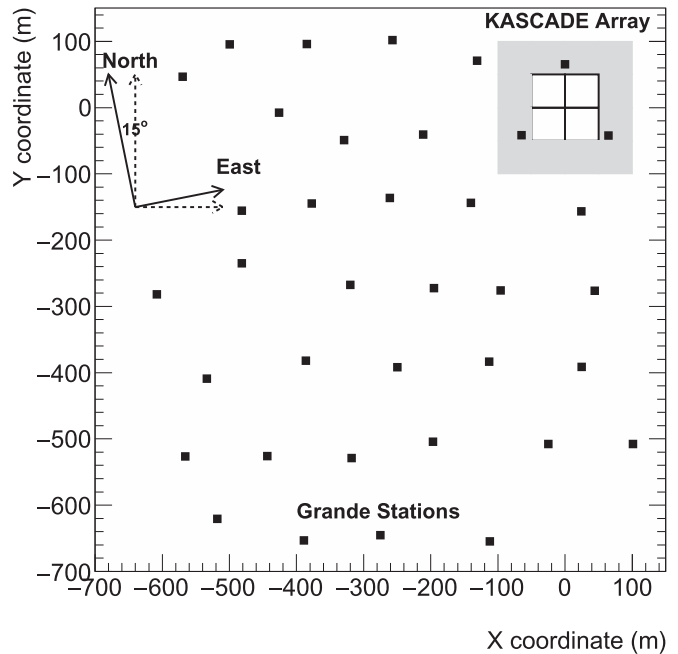


Figure 1. Layout of the KASCADE-Grande experiment.

The uncertainties on r_I and ψ_I depend on the total number of counts N and δt and are equal to:

$$\sigma_{r_I} = \frac{1}{\delta t} \sqrt{\frac{2}{N}},$$

$$\sigma_{\psi_I} = \frac{\sigma_{r_I}}{r_I}.$$

The probability that this amplitude is due to a statistical fluctuation of background can be calculated with the Rayleigh probability:

$$P = \exp\left(-\frac{r_I^2}{2\sigma_{r_I}^2}\right). \quad (5)$$

In this work we report on a search for large-scale anisotropies performed by applying the east–west method to the KASCADE-Grande data.

2. The Experiment

The multidetector experiment KASCADE (Antoni et al. 2003; located at 49.1°N, 8.4°E, 110 m a.s.l.) was extended to KASCADE-Grande (Apel et al. 2010) in 2003 by installing a large array of 37 stations (named Grande) that consist of 10 m² plastic scintillation detectors each (Figure 1). KASCADE-Grande provided an active area of about 0.5 km² and operated jointly with the existing KASCADE detectors. The data taking ended in 2013 January. The Grande array was installed on an irregular triangular grid with an average spacing of 137 m; for triggering purposes the stations were organized in 16 hexagons with 6 stations at the edges and 1 in the center. The shower trigger was given by the full coincidence of the seven modules of a single hexagon. The analysis discussed in this article is based on the data recorded by the Grande array, and the data of

the muon detectors, located at the KASCADE field, are not used in this work.

The arrival direction of individual events is obtained by fitting the particles' arrival time measured by the 37 Grande stations. The core location, the slope of the lateral distribution function, and the shower size (i.e., the total number of charged particles, N_{ch}) are the result of a maximum likelihood fit comparing the measured number of particles with the one expected from an NKG-like (Nishimura Kamata Greisen) lateral distribution function (Apel et al. 2006) of the charged particles in the shower.

KASCADE-Grande provides the unique opportunity to evaluate the reconstruction accuracies of the Grande array with a direct comparison with an independent experiment (KASCADE). For a subsample of events the two independent reconstructions of the KASCADE and the Grande arrays are compared. We derive that the Grande reconstruction accuracies, in the region of 100% reconstruction and detection efficiency, are: $\leq 15\%$ for N_{ch} (with a systematic shift in respect to KASCADE $\leq 5\%$), $\sim 0.8^\circ$ for the arrival direction, and ~ 6 m for the core position.

A detailed description of the event reconstruction and performance of the Grande array can be found in Apel et al. (2010).

2.1. Data Selection

The number of counts from the east- and westward sectors are affected by a trigger inefficiency in the same way; therefore, the east–west method can be also applied to data collected with trigger conditions that do not reach a 100% efficiency. No selection cuts are applied on the core position, and all the events with zenith angle of $\theta \leq 40^\circ$ and shower size of $N_{\text{ch}} \geq 10^{5.2}$ are used in this analysis.

In this analysis we have chosen the average hour angle between the vertical and the east and westward sectors: $\delta t \sim 20^\circ$.

The primary energy is estimated from the shower size $N_{\text{ch}}(\theta)$, which is converted (by applying the constant intensity cut technique; Hershil et al. 1961) to its value at a reference zenith angle ($\theta_{\text{ref}} = 20^\circ$). The primary energy is then evaluated using the calibration function obtained (Kang et al. 2013) for primary protons by means of a complete EAS simulation based on the QGSJetII-02 hadronic interaction model (Ostapchenko 2006). The systematic error in the energy assessment due the choice of the specific hadronic interaction model is around 20% (Apel et al. 2014). The values of the amplitude and the phase of the first harmonics will be referred to the median energy of the event sample. The conversion from $N_{\text{ch}}(\theta_{\text{ref}})$ to energy has been calculated for primary protons; therefore, the energy we estimate is a lower limit of the true one, as the chemical composition of real events is heavier than pure protons.

Considering the number of events accumulated by the KASCADE-Grande experiment we divide a day into $n_{\text{int}} = 72$ intervals (i.e., 20 minutes). The distribution of the number of events in solar time is shown by the solid line in Figure 2; large fluctuations, due to spurious anisotropies introduced by atmospheric and instrumental effects, are present. The dashed line shows the same distribution obtained by applying the east–west method; the previously seen spurious fluctuations are removed.

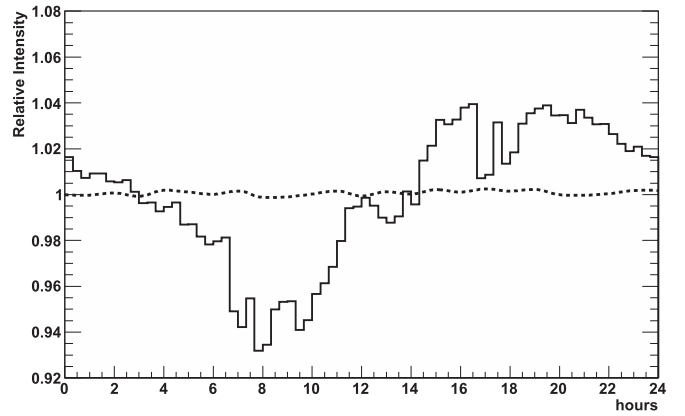


Figure 2. Comparison of the local solar time count variations measured by the KASCADE-Grande experiment (solid line) with those obtained by applying Equation (4) (dashed line).

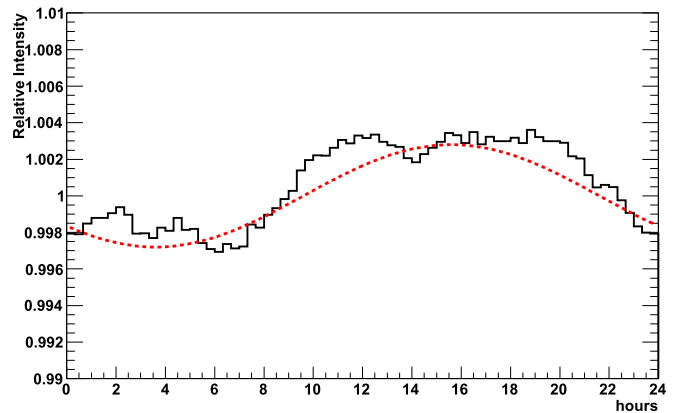


Figure 3. Sidereal time variations of the number of counts obtained, in 20 minutes intervals, by applying the east–west method. The dashed line represent the first harmonic fit; the amplitude and phase values are reported in Table 1.

Table 1
Results of First Harmonic Analysis (Amplitude, Phase, and Rayleigh Probability) in Sidereal, Solar, and Anti-sidereal Time

Time	$A \times 10^{-2}$	Hours	P
Sidereal	0.28 ± 0.08	15.1 ± 1.1	0.2%
Solar	0.15 ± 0.08	23.9 ± 2.1	17%
Anti-sidereal	0.02 ± 0.08	1.8 ± 14.4	96%

3. Results and Discussion

We can, therefore, apply the east–west method to obtain the number of counts distributions (20 minutes bin width, corresponding to an angular aperture of 5°) in solar, sidereal (shown in Figure 3), and anti-sidereal times. These distributions are fitted with a first harmonic function, and the values of the amplitudes and phases are reported in Table 1 together with the Rayleigh probability owing to background fluctuation. As expected only the amplitude of the sidereal time distribution shows a small Rayleigh probability value ($P = 0.2\%$); nevertheless its significance is 3.5σ and, therefore, we calculate (according to the distribution drawn from a population characterized by an anisotropy of unknown amplitude and phase as derived by Linsley 1975), the 99% confidence level upper limit to the amplitude: $A \leq 0.47 \times 10^{-2}$.

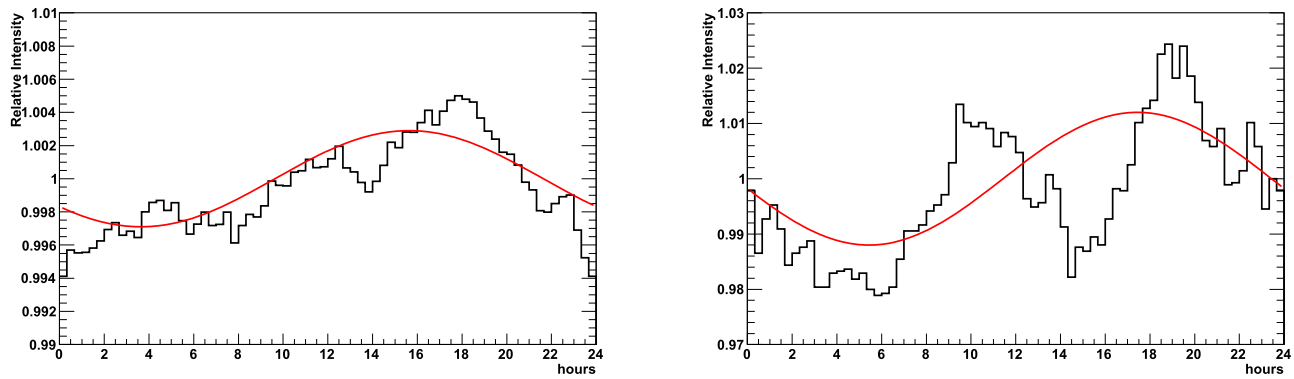


Figure 4. Sidereal time variations of the number of counts obtained in the $10^{5.6} < N_{\text{ch}} < 10^{6.4}$ (left panel) and $N_{\text{ch}} > 6.4$ (right panel) shower size intervals by applying the east–west method ($\Delta t = 20$ minutes). The line represent the fitted first harmonic; amplitudes and phases are reported in Table 2.

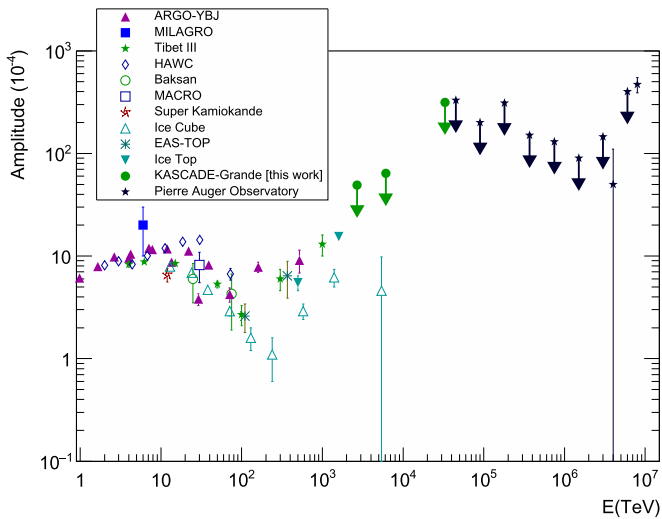


Figure 5. Comparison of the upper limits to the amplitude of the first harmonic obtained by KASCADE-Grande with experimental results in the energy range of $10^{13} < E < 10^{19}$ eV. References to other experiments data are: Ambrosio et al. (2003), Amenomori et al. (2005, 2017), Guillian et al. (2007), Abdo et al. (2009), Aglietta et al. (2009), Alekseenko et al. (2009), Abbasi et al. (2010, 2012), Aartsen et al. (2013), Bartoli et al. (2015b, 2018), Aab et al. (2017), and Abeysekara et al. (2018).

The values in Table 1 have been obtained with the full KASCADE-Grande data set; therefore, we cannot expect significant amplitudes dividing the event sample in energy intervals. We nevertheless perform this search to investigate the behavior of the phase with energy. The previously discussed analysis is repeated in three intervals of N_{ch} : $5.2 \leq \log N_{\text{ch}} \leq 5.6$, $5.6 \leq \log N_{\text{ch}} \leq 6.4$, and $\log N_{\text{ch}} \geq 6.4$. In Figure 4 the sidereal time distributions of the number of counts, obtained in the two highest N_{ch} intervals, are shown. The first harmonic amplitude and phase values are reported in Table 2 together with the median energies. The significance of the first harmonic amplitude decreases (as shown by the Rayleigh probability in Table 2), increasing the charged particles number. Correspondingly the phase is obtained with a larger uncertainty. We calculate the 99% confidence level upper limits of the first harmonic amplitude for the three energy intervals: $A \leq 0.49 \times 10^{-2}$, $A \leq 0.64 \times 10^{-2}$, and $A \leq 3.15 \times 10^{-2}$ (shown in Figure 5).

Figures 5 and 6 show a comparison of the results of this work with those obtained at lower and higher energies by other

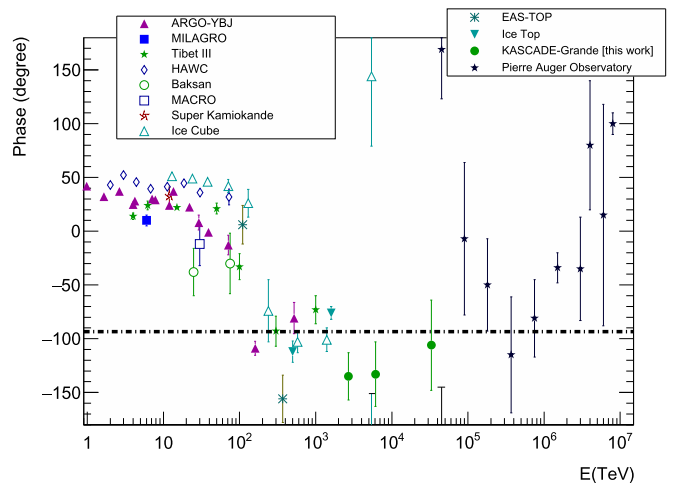


Figure 6. Comparison of the KASCADE-Grande measurements of the phase of the first harmonic with experimental results obtained in the energy range of $10^{13} < E < 10^{19}$ eV. The dotted line shows the direction of the galactic center. The references to the results of the other experiments can be found in the caption of Figure 5.

experiments (see Ahlers & Mertsch 2017 and references therein).

The first harmonic phases measured by the KASCADE-Grande experiment agree with those measured by EAS-TOP (Aglietta et al. 2009), IceCube (Aartsen et al. 2016) and IceTop (Aartsen et al. 2013) at energies greater than 2×10^{14} eV, showing that the change of phase, in the direction of the galactic center, observed at $E \sim 2 \times 10^{14}$ eV also holds at energies greater than the knee of the cosmic-ray spectrum.

These results fill the gap between the experiments studying the knee and the ankle of the cosmic-ray spectrum. The phase of the first harmonic shows a first change from $\sim 30^\circ$ to $\sim -140^\circ$ at energies slightly above 10^{14} eV, then it remains constant until $< 10^{17}$ eV, and (as recently shown by the Pierre Auger Observatory; Aab et al. 2017), changes to $\sim 100^\circ$ around 8×10^{18} eV. The phase flip of the dipole anisotropy observed around 0.1–0.3 PeV may indicate (Ahlers 2016) the change from a galactic cosmic-ray emission dominated, below these energies, by few local sources to a source distribution pointing to the galactic center region. The second phase flip observed above 10^{18} eV can be interpreted as the sign of an extra galactic origin of ultra high-energy cosmic rays (Aab et al. 2017).

Table 2
First Harmonic Amplitude and Phase in Different Intervals of N_{ch}

$\text{Log}(N_{\text{ch}})$	Median Energy (eV)	$A \times 10^{-2}$	Phase (deg)	P	Number of Events	U.L. (99% c.l.)
5.2–5.6	2.7×10^{15}	0.26 ± 0.10	225 ± 22	3%	1.42×10^7	0.49×10^{-2}
5.6–6.4	6.1×10^{15}	0.29 ± 0.16	227 ± 30	19%	6.27×10^6	0.64×10^{-2}
≥ 6.4	3.3×10^{16}	1.2 ± 0.9	254 ± 42	41%	1.97×10^5	3.15×10^{-2}

This paper is dedicated to Bogdan Mitrica, a long-time member of the KASCADE-Grande Collaboration, who unfortunately died far too young in October 2018. The authors would like to thank the members of the engineering and technical staff of the KASCADE-Grande collaboration, who contributed to the success of the experiment. The KASCADE-Grande experiment is supported in Germany by the BMBF and by the ‘‘Helmholtz Alliance for Astroparticle Physics—HAP’’ funded by the Initiative and Networking Fund of the Helmholtz Association, and by the MIUR and INAF of Italy, the Polish Ministry of Science and Higher Education, and the Romanian Authority for Scientific Research UEFISCDI (PNII-IDEI grants 271/2011 and 17/2011). J.C.A.V. acknowledges the partial support of CONACyT and the Coordinaci3n Científica de la Universidad Michoacana.

ORCID iDs

A. Chiavassa  <https://orcid.org/0000-0001-6183-2589>

References

- Aab, A., Abreu, P., Aglietta, M., et al. 2017, *Sci*, **357**, 1266
Aartsen, M. G., Abbasi, R., Abdou, Y., et al. 2013, *ApJ*, **765**, 55
Aartsen, M. G., Abraham, K., Ackermann, M., et al. 2016, *ApJ*, **826**, 220
Abbasi, R., Abdou, Y., Abu-Zayyad, T., et al. 2010, *ApJL*, **718**, L194
Abbasi, R., Abdou, Y., Abu-Zayyad, T., et al. 2012, *ApJ*, **746**, 33
Abdo, A. A., Allen, B. T., Aune, T., et al. 2009, *ApJ*, **698**, 2121
Abeyssekara, A. U., Alfaro, R., Alvarez, C., et al. 2018, *ApJ*, **865**, 57
Aglietta, M., Alessandro, B., Antonioli, P., et al. 2004, *Aph*, **21**, 223
Aglietta, M., Alekseenko, V. V., Alessandro, B., et al. 2009, *ApJL*, **692**, L130
Ahlers, M. 2016, *PhRvL*, **117**, 151103
Ahlers, M., & Mertsch, P. 2017, *PrPNP*, **94**, 184
Alekseenko, V. V., Cherniaev, A.B., Djappuev, D.D., et al. 2009, *NuPhS*, **196**, 179
Ambrosio, M., Antolini, R., Baldini, A., et al. 2003, *PhRvD*, **67**, 042002
Amenomori, M., Ayabe, S., Cui, S.W., et al. 2005, *ApJL*, **626**, L29
Amenomori, M., Bi, X. J., Chen, D., et al. 2017, *ApJ*, **836**, 153
Antoni, T., Apel, W. D., Badea, F., et al. 2002, *Aph*, **16**, 373
Antoni, T., Apel, W. D., Badea, F., et al. 2003, *NIMPA*, **513**, 429
Apel, W. D., Arteaga, J. C., Badea, A. F., et al. 2010, *NIMPA*, **620**, 202
Apel, W. D., Arteaga-Velazquez, J. C., Bekk, K., et al. 2011, *PhRvL*, **107**, 171104
Apel, W. D., Arteaga-Velazquez, J. C., Bekk, K., et al. 2014, *AdSpR*, **53**, 1456
Apel, W. D., Badea, A. F., Bekk, K., et al. 2006, *Aph*, **24**, 467
Bartoli, B., Bernardini, P., Bi, X. J., et al. 2015a, *PhRvD*, **92**, 092005
Bartoli, B., Bernardini, P., Bi, X. J., et al. 2015b, *ApJ*, **809**, 90
Bartoli, B., Bernardini, P., Bi, X. J., et al. 2018, *ApJ*, **861**, 93
Bonino, R., Alekseenko, V. V., Deligny, O., et al. 2011, *ApJ*, **738**, 67
Guillian, G., Hosaka, J., Ishihara, K., et al. 2007, *PhRvD*, **75**, 062003
Hersil, J. I., Escobar, I., Scott, D., Clark, G., & Olbert, S. 1961, *PhRvL*, **6**, 22
Kang, D., Apel, W. D., Arteaga-Velazquez, J.C., et al. 2013, *J. Phys.: Conf. Ser.*, **409**, 012101
Linsley, J. 1975, *PhRvL*, **34**, 1530
Ostapchenko, S. 2006, *PhRvD*, **74**, 014026